

Conversion of the E1A Cys₄ zinc finger to a nonfunctional His₂Cys₂ zinc finger by a single point mutation

(E1A trans-activation/site-directed mutagenesis/atomic absorption spectrophotometry/x-ray absorption fine structure analysis)

LELAND C. WEBSTER*[†], KE ZHANG[‡], BRITTON CHANCE[‡], IRAIMOUDI AYENE[‡], JEFFREY S. CULP[§], WEI-JEN HUANG[¶], FELICIA Y.-H. WU[¶], AND ROBERT P. RICCIARDI*^{***}

[‡]Institute for Structural Functional Studies, Philadelphia, PA 19104; [§]Department of Protein Biochemistry, SmithKline and Beecham Pharmaceuticals, King of Prussia, PA 19406; [¶]Department of Pharmacological Sciences, School of Medicine, State University of New York, Stony Brook, NY 11794; and *The Wistar Institute of Anatomy and Biology, 3601 Spruce Street, Philadelphia, PA 19104

Contributed by Britton Chance, August 12, 1991

ABSTRACT Trans-activation by the adenovirus E1A 289R protein requires a zinc finger defined by Cys-154, Cys-157, Cys-171, and Cys-174. Whereas individually replacing the four cysteine residues with serines resulted in a loss of trans-activation, only three of the Cys → Ser mutants (C157S, C171S, and C174S) lost the ability to bind Zn(II). X-ray absorption fine structure analysis revealed that, in the wild-type protein, Zn(II) is coordinated by four cysteine residues whereas in the C154S mutant, Zn(II) is coordinated by two histidines and two cysteines. The mutant protein probably retains, as ligands, two cysteines on the right side of the zinc finger (Cys-171 and Cys-174) and recruits two of the four histidines on the left side (His-149, His-152, His-158, and His-160), despite the presence of Cys-157. This finding may shed light on the general structural requirements of zinc fingers.

Zinc fingers represent a class of eukaryotic DNA binding structures found in a variety of gene regulatory proteins, typically occurring as tandem repeats. There are two major types of zinc finger, C₂H₂ and C₄, which are formed by the folding of a 20- to 30-amino acid region around a single zinc ion coordinated by two cysteines and two histidines or by four cysteines, respectively (1, 2). Mutational analyses of many zinc fingers have demonstrated their importance in transcriptional regulation (3–7). Physical analyses of a limited number of these proteins have confirmed that the predicted metal-binding ligands indeed coordinate Zn(II) (8–12) and, for the yeast ADR1, *Xenopus* Xfin, and rat glucocorticoid receptor proteins, three-dimensional finger structures have been obtained through nuclear magnetic resonance (13–15).

The adenovirus E1A 289R protein trans-activates early viral promoters (16, 17) and some cellular promoters (18, 19). Although the ability to bind DNA has been definitively demonstrated for several zinc finger proteins [e.g., TFIIIA (20), SP1 (21), ADR1 (22), SW15 (23), and the glucocorticoid receptor (24)], the E1A 289R protein does not bind to DNA in a sequence-specific manner (25, 26). However, the E1A zinc finger, which resides within a conserved stretch of 46 amino acids, is required for the trans-activating function (27–29). Although the mechanism by which the 289R protein trans-activates E1A-inducible promoters is unclear, there is strong evidence suggesting that E1A acts through cellular transcription factors (30–35). Moreover, there is convincing genetic evidence that the E1A zinc finger itself binds a cellular factor (53).

The E1A 289R protein contains a predicted C₄ zinc finger motif, C¹⁵⁴-X₂-C¹⁵⁷-X₁₃-C¹⁷¹-X₂-C¹⁷⁴ (36). The four cysteines were implicated in metal coordination, since (i) the binding of

a single zinc ion was mapped to the trans-activating domain and (ii) individually replacing each cysteine with glycine destroyed trans-activation (37). The more conservative Cys-154 → Ser substitution (C154S) also resulted in loss of trans-activation (37). We predicted that if these cysteine residues were bona fide ligands, then the mutant proteins would not bind Zn(II). Surprisingly, the purified C154S protein produced in a bacterial expression system binds one Zn(II) as tightly as the wild-type 289R protein (37). This called into question the identity of the exact wild-type ligands.

The results presented here support the hypothesis that the predicted C₄ finger structure in the E1A trans-activating domain is indeed the Zn(II) binding site. Furthermore, we show that the ability of the C154S protein to bind zinc results from the recruitment of two histidines in place of two normally used ligands (Cys-157 and Cys-154), creating an H₂C₂ zinc finger. These results verify that E1A trans-activation requires a specific C₄ zinc finger structure.

MATERIALS AND METHODS

Plasmids and Transfections. The wild-type E1A plasmid pSK-E1A was constructed by subcloning the *EcoRI*-*Kpn* I fragment of the 13S cDNA eukaryotic expression plasmid pJN20 (38) into the polylinker site of the pBluescript SK(-) (Stratagene). The p3CAT plasmid contains the chloramphenicol acetyltransferase (CAT) gene driven by the E3 promoter of adenovirus 5 (39). HeLa cells were cotransfected with E1A plasmids and the reporter plasmid p3CAT, as described (27). Cells were harvested after 40 hr and extracts were assayed for CAT activity as described (40).

Mutagenesis. Oligonucleotide-directed mutagenesis was performed using Amersham mutagenesis reagents by the method of Nakamaye and Eckstein (41). Mutants C154S, C157S, C171S, and C174S were generated by changing codons 154 (TGC to AGC), 157 (TGT to TCT), 171 (TGT to TCT), and 174 (TGC to TCC), respectively. Mutations were verified by DNA sequencing (42).

Overexpression of E1A Proteins in *Escherichia coli*. For expression of full-length proteins in bacteria, the 216-base-pair *Sma* I-*Xba* I fragments of the pSK-E1A mutants were subcloned into the E1A bacterial expression vector pAS1-E1A410 (43). The proteins were overexpressed in *E. coli*

Abbreviations: CAT, chloramphenicol acetyltransferase; XAFS, x-ray absorption fine structure; RDF, radial distribution function; Im, imidazole.

[†]Present address: Department of Biology, Chemistry and Molecular Pharmacology, Harvard Medical School, 240 Longwood Avenue, Boston, MA 02115.

[¶]Present address: Institute of Biomedical Sciences, Academia Sinica, Taipei 11529, Taiwan, Republic of China.

^{***}To whom reprint requests should be addressed.

The publication costs of this article were defrayed in part by page charge payment. This article must therefore be hereby marked "advertisement" in accordance with 18 U.S.C. §1734 solely to indicate this fact.

AR120, purified to near homogeneity, charged with Zn(II), and analyzed for Zn(II) content using a Perkin-Elmer model 4000 atomic absorption spectrophotometer equipped with a HGA 400 graphite furnace as described (37).

X-Ray Absorption. Proteins for x-ray absorption fine structure (XAFS) measurement were purified and charged with Zn(II) in the manner described for atomic absorption experiments (37). Proteins were made ≈ 1.0 mM, final concentration, by repeated centrifugations at $1500 \times g$, 4°C in an Amicon Centriprep-30 and at $300 \times g$, 25°C in a Centricon-30. To prevent protein aggregation in the Centricon-30 as the final concentration was approached, the protein gradient was disrupted by pipetting after each 10-min centrifugation. Protein concentrations were determined using the method of Bradford (44). X-ray absorption experiments were carried out on Beamline X9-A of the National Synchrotron Light Source at Brookhaven National Laboratory with a constant exit height double crystal monochromator with Si(111) crystals. A nickel-coated mirror was used to reject the third-order harmonics by adjusting the angle of the mirror relative to the incident beam. A 13-element intrinsic Ge detector was used to detect the Zn(II) K_α fluorescence from the sample generated by the absorption of the x-ray beam. Series of scans were collected for both the C154S mutant and the wild-type proteins at a sample temperature of 130 K, for a total of several million signal counts. XAFS data for model compounds were also collected in the fluorescence mode using both the Ge detector and an ionization chamber (Stern/Heald type). ZnS was ground, sieved (400 mesh), and spread uniformly onto Scotch tape for the measurement. $[\text{Zn}(\text{NH}_3)_4]^{2+}$, hereafter referred to as $\text{Zn}(\text{NH}_3)_4$, was made by dissolving $\text{Zn}(\text{NO}_3)_2$ in distilled water, precipitating $\text{Zn}(\text{OH})_2$ with 5% (wt/vol) ammonium hydroxide, and dissolving the precipitate in 30% (wt/vol) ammonium hydride. The $[\text{Zn}(\text{Im})_4](\text{ClO}_4)_2$ complex, hereafter referred to as $\text{Zn}(\text{Im})_4$ (where Im is imidazole), was prepared by combining $\text{Zn}(\text{ClO}_4)_2$ with a 6-fold excess of Im. The concentrations of the solution model compound [namely, $\text{Zn}(\text{NH}_3)_4$ and $\text{Zn}(\text{Im})_4$] used for XAFS measurement were between 10 mM and 15 mM.

RESULTS AND DISCUSSION

To resolve to what extent the E1A consensus finger sequence is involved in Zn(II) binding, we individually substituted serine for three cysteine residues (Cys-157, Cys-171, and Cys-174), as was done for Cys-154 (37) (Fig. 1) and tested each mutant protein for its ability to trans-activate and bind Zn(II). Site-directed mutagenesis was performed on a plasmid containing an E1A promoter-driven cDNA, pSK-E1A, that encodes the E1A 289R protein. These mutants were tested for their ability to trans-activate the E1A-inducible E3 promoter linked to the CAT reporter gene after transient plasmid cotransfection into HeLa cells. Like C154S (37), these conservative substitutions destroyed trans-activation (Table 1). Western blot analysis confirmed that similar amounts of the mutant and wild-type E1A proteins were synthesized in the transiently transfected HeLa cells (data not shown). Therefore, the lack of trans-activation by any of the mutant proteins could not be attributed to decreased polypeptide stability.

Since C154S fails to trans-activate, yet binds Zn(II) as tightly as the wild-type protein (37), we asked whether the other trans-activation-defective mutants C157S, C171S, and C174S would retain the ability to bind Zn(II). We cloned these mutated E1A sequences into the bacterial expression plasmid pAS1-E1A410. Mutant E1A proteins were overexpressed in *E. coli* and purified to near homogeneity, and the Zn(II) content was determined by atomic absorption spectrophotometry. In contrast to wild-type E1A and C154S, the following are not able to bind Zn(II): C157S, C171S, and C174S (Table 1). Since histidine can also bind Zn(II), a likely

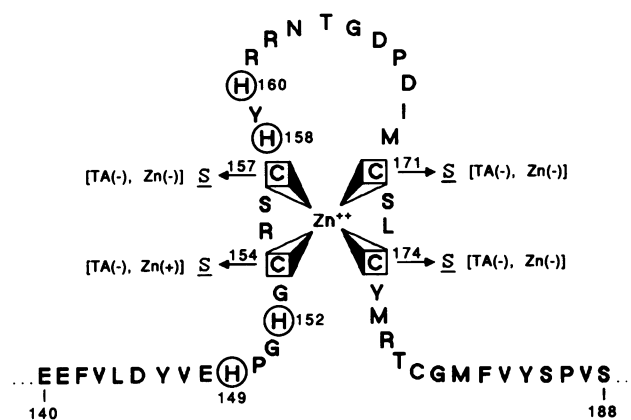


FIG. 1. Schematic representation of the E1A zinc finger structure and the effects of individual Cys \rightarrow Ser substitutions. The trans-activating region of adenovirus 5 E1A (residues 140–188) is shown. All four Cys \rightarrow Ser mutants fail to trans-activate, TA(-), and fail to bind zinc, Zn(-), except for C154S, which binds zinc, Zn(+). The XAFS data indicate that Zn(II) in the wild-type protein is bound by the four highlighted cysteines whereas in C154S Zn(II) is bound by two cysteines and two histidines. This coordination by the C154S protein probably involves two of the four circled histidines and Cys-171 and Cys-174.

explanation for Zn(II) binding to C154S may lie in the potential of neighboring histidines (His-149, His-152, His-158, and His-160) to function as alternate ligands. On the other hand, the actual zinc ligands in the wild-type 289R protein may be different from the predicted ligands [i.e., instead of Cys-154, the following may bind Zn(II) in conjunction with C157S, C171S, and C174S: His-149, His-152, His-158, and His-160]. To resolve these possibilities, we performed XAFS experiments on both the wild-type and the mutant C154S E1A proteins. XAFS can reveal both the types and the number of atoms involved in metal coordination.

The XAFS data were analyzed by the standard procedure (45–47). Fig. 2A shows the XAFS $\chi(k)$ data for the wild-type and C154S mutant E1A after E (energy) to k (photoelectron wave number) conversion, atomic background subtraction, and normalization. Fig. 2B shows the Fourier transform of the χ data between 1 and 12 \AA^{-1} in k -space. The contribution of the first coordination shell of Zn(II) was isolated using an R -space window 1.6 \AA wide. The data show a clear distinction between the wild-type and the mutant proteins.

The single-shell data were quantitatively analyzed using the least-squares fitting method. Since sulfur and nitrogen bind Zn(II) at distinct distances, models can be designed that correspond to different ligand combinations. Therefore, one

Table 1. Analysis of function and Zn(II) content of mutant E1A proteins

E1A protein	Trans-activation	Zn(II) content
Wild type	1.0	0.96*
C154S	<0.1	1.04*
C157S	<0.1	0.05
C171S	<0.1	0.05
C174S	<0.1	0.05

HeLa cells were cotransfected with E1A plasmids and the reporter plasmid p3CAT. Cell extracts were assayed for CAT activity 40 hr after transfection. Wild-type activity is arbitrarily defined as 1.0. Zn(II) content values represent mol of Zn(II) per mol of protein; error values for wild-type and C154S were ± 0.1 and for C157S, C171S, and C174S were ± 0.05 . Proteins were overexpressed in *E. coli* AR120, purified to near homogeneity, charged with Zn(II), and analyzed by atomic absorption spectrophotometry.

*Values for the zinc content of the wild-type and the C154S proteins have been reported (37).

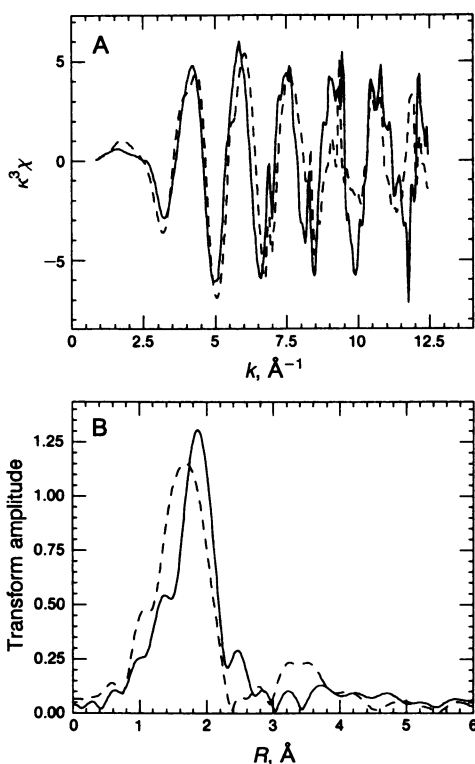


FIG. 2. Zn K-edge XAFS raw data (A) and its Fourier transform (B) of wild-type E1A protein and mutant C154S E1A proteins. The wild-type protein is represented by a solid line and the mutant protein by a dashed line. The XAFS data are plotted as $\kappa^3\chi(k)$, where $\chi(k)$ is obtained by removing the atomic absorption background from the absorption spectra with a cubic spline fit, converting from energy space to k -space and normalizing with a constant edge step. The Fourier transform was performed from 1 to 12 \AA^{-1} . The first coordination shell was isolated by inverse Fourier transform with a window from 0.8 to 2.4 \AA in R -space.

and two distance models were used in which the coordination numbers, the distances, and the Debye–Waller factors could be varied. The fitting was performed between 1.8 and 10 \AA^{-1} in k -space for both the wild-type and the mutant proteins. This gives about eight degrees of freedom in the data range (48). The quality of a fit, Q , can be measured (49) as follows:

$$Q = \frac{1}{N - P} \sum_i \frac{(\sigma_i^f)^2}{(\sigma_i^y)^2}, \quad [1]$$

where σ_i^f is the combined phase and amplitude error of the fit at point i , and σ_i^y is the error introduced by the measurement and data analysis procedure. σ_i^y can be estimated from the variation of different scans of measurement and the non-transferability error of the standards from analysis of model compounds of known structure. N is the independent data points included within the data range to be modeled (48), and P is the number of parameters used in the fit. A fit with Q value less than or close to unity can be accepted; otherwise, it is rejected. This fitting criterion (49), which incorporates the variation of statistical and systematic errors in k -space and the number of degrees of freedom in the data range, was used to distinguish between the fitting models.

The results for the best fits and the Q values of the wild-type and the mutant proteins are presented in Table 2, along with the fitting results of other possible models. The wild-type E1A data were adequately fitted by the single distance model (Fig. 3A). Inclusion of both sulfur and nitrogen atoms in the fit increased the Q value, making the fit unacceptable according to the criterion. The first shell of

Table 2. Fitting results for various models for the first shell of E1A proteins

E1A protein	Model	Atom	N	R , \AA	σ^2 , \AA^2	Q status
Wild type	1	S	4.2 (5)	2.34 (1)	0.000	0.6
	2	S	3	2.34	-0.002	3.0
		N	1	2.01	0.015	
C154S mutant	1	S	2	2.33 (2)	-0.001	1.1
		N	2	2.01 (2)	-0.001	
	2	S	3	2.32	0.002	2.3
		N	1	2.00	-0.004	

Values in the parentheses are the error in the last digit.

Zn(II) in the wild-type E1A protein contains 4.2 ± 0.5 sulfur atoms at a distance of 2.34 \AA . This is consistent with the hypothesis that the Zn(II) is bound by four cysteines. For the mutant E1A protein, however, a single distance fit was not sufficient and the experimental data were best fit with two nitrogens located at 2.01 ± 0.02 \AA and two sulfurs at 2.33 ± 0.02 \AA (Fig. 3B). Fitting with three sulfurs and one nitrogen increased the Q value (Table 2), making the fit unacceptable.

We verified the fitting results by using the "splice" method (refs. 50 and 51; E. A. Stern, personal communication) to generate the radial distribution function (RDF) around the

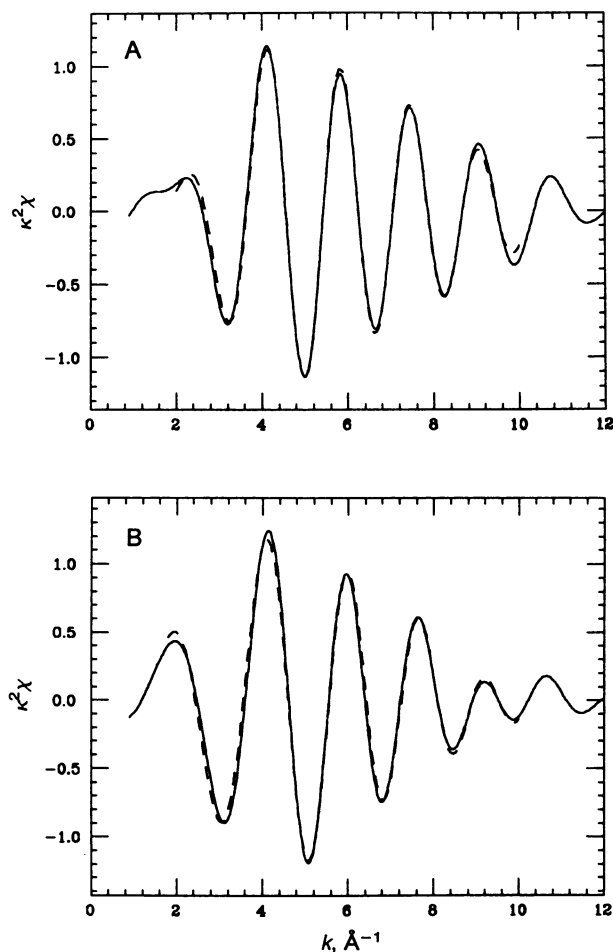


FIG. 3. Least-squares fitting results. (A) First-shell $\chi(k)$ data of the wild-type E1A protein (solid line) compared with the single distance fit using ZnS as model compound (dashed line). The data can be adequately fitted with 4.2 ± 0.5 sulfur atoms at a distance of 2.34 ± 0.02 \AA from the Zn(II). (B) First-shell $\chi(k)$ data (solid line) of the C154S mutant protein compared with the two distance fit (dashed line) using ZnS and Zn(Im)₄ or Zn(NH₃)₄ as sulfur and nitrogen model compounds, respectively. The data were fitted with two sulfurs at 2.33 ± 0.02 \AA and two nitrogens at 2.02 ± 0.02 \AA .

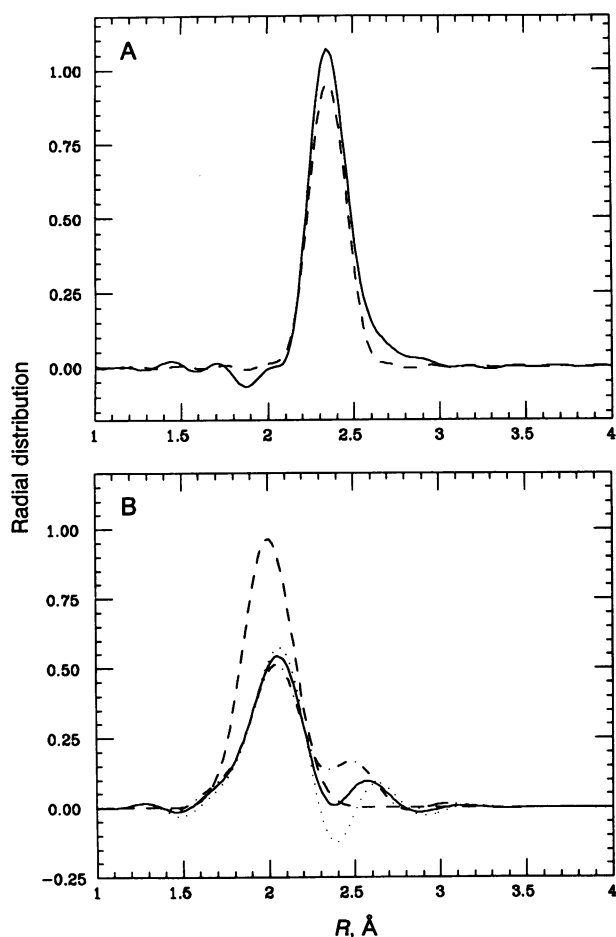


FIG. 4. RDF results. (A) The RDF of the wild-type protein generated using the "splice" method is shown as the solid line, which is compared with the RDF of ZnS (dashed line) generated from the known structure. The RDF is consistent with the fitting results. The distribution was artificially broadened by a Gaussian factor of $\sigma_c^2 = 0.001 \text{ \AA}^2$ to reduce the truncation ripple due to lack of high k information. (B) The RDF was generated by subtracting out one sulfur (dotted line), two sulfur (solid line), and three sulfur (dot-dashed line) contributions, compared with the known distribution of Zn(NH₃)₄ (dashed line). The trough or peak at 2.4 \AA for the subtractions of one and three Zn(II)-S pairs, which is close to the distance of Zn(II)-S pair, is probably due to under- or oversubtraction of Zn(II)-S pairs. Since the backscattering phase difference between nitrogen and sulfur is about π , undersubtraction will make a trough when dividing by the nitrogen model; oversubtraction will make a peak. The RDF data indicate that the model with two sulfurs and two nitrogens as the first neighbors is correct. To minimize truncation effects, the distributions were artificially broadened by a Gaussian factor of $\sigma_c^2 = 0.02 \text{ \AA}^2$.

zinc ion. This method, which is not widely known, has the advantage over the least-squares fitting method of not requiring an assumed form for the distribution of atoms. Briefly, the backscattering amplitude and the central and backscattering phase are removed by taking the amplitude ratio and phase difference between the filtered XAFS $\chi(k)$ function of the unknown and an appropriate model. The amplitude ratio and the phase difference are then extrapolated through the low k (electron wave number) region using the cumulant expansion (47). The RDF is obtained by inverting the data with a Fourier transform with a Gaussian damping factor to minimize artifacts from truncating the data at high k . Artificial broadening of the RDF occurs as a side-effect of this truncation.

The RDF generated for the wild-type E1A protein is compared with RDF of ZnS in Fig. 4A. The ratio of the areas

of the distributions, which are proportional to the coordination numbers, is about 1.1 between the wild-type E1A and ZnS, indicating that four sulfurs are the first-shell ligands. The central position of the distribution is 2.34 \AA , consistent with the fitting results.

The RDF cannot be generated automatically for the mutant, since the first coordination shell is a mixture of two kinds of atoms. However, the RDF of nitrogen in the first shell can be obtained if the contribution of Zn(II)-S pairs is subtracted out. Fig. 4B shows the RDFs of the mutant E1A protein with one, two, and three Zn(II)-S pair contribution subtracted out, compared with the RDF of model compound Zn(NH₃)₄. Two nitrogens (± 0.1) were found in the first shell with an average distance of 2.02 \AA in all three cases. The two distributions corresponding to subtractions of one and three Zn(II)-S pairs have a trough or peak, respectively, located at about 2.4 \AA , and the distribution for the subtraction of two Zn(II)-S pairs has a peak at about 2.6 \AA . The trough or peak located at 2.4 \AA can be attributed to under- or oversubtraction of Zn(II)-S contributions (Fig. 4). On the other hand, the subtraction of two Zn(II)-S pairs is adequate, due to the disappearance of the 2.4- \AA peak or trough. The smaller peak at 2.6 \AA evident in the subtraction of the two Zn(II)-S pairs is presumably due to neighboring atoms that were included in the back transform window. Indeed, the same peak occurs for the RDF of Zn(Im)₄ using the same back transform window. The RDF analysis shows that the zinc ion in the C154S protein is bound to two nitrogens and two sulfurs, confirming the fitting results.

The contribution of the γ -carbon and δ_1 -nitrogen of the histidine located 4.2 \AA from the metal site is enhanced about 3-fold due to the focusing effect (52). The higher coordination shell was analyzed for evidence of histidine ligands. This contribution was isolated using a back transform window of 2.8–4.2 \AA and compared with the zinc Im model compound. As shown in Fig. 5, the mutant data could be fitted with 2 (± 0.4) Im contributions (one γ -carbon and one σ_1 -nitrogen each) at an average distance 0.04 \AA greater than in the model compound. This is consistent with the finding that two histidines are in the first coordination sphere of the zinc ion.

There are two major classes of zinc fingers in regulatory proteins, C₄ and C₂H₂. Our results show definitively that E1A is a C₄ type finger. Whereas individual replacement of the four cysteines with serine destroys trans-activation, the C154S protein is unique in that it retains the ability to bind Zn(II) (37). Because there are neighboring histidines only on the amino-terminal side of the E1A zinc finger (Fig. 1) that

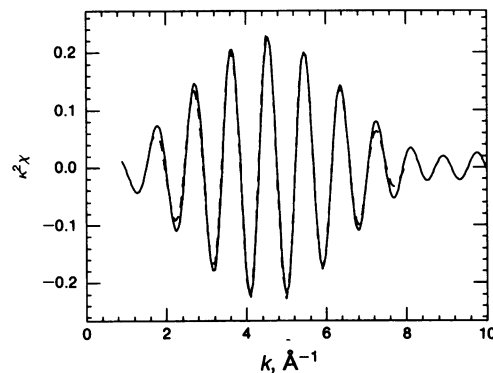


FIG. 5. XAFS $\chi(k)$ data of the third shell of the mutant protein (solid line) and its fit (dashed line). The contribution was isolated between 2.8 and 4.2 \AA in the Fourier transform as in Fig. 2. The signal is due to γ -carbon and δ_1 -nitrogen of the Im ring and is enhanced by the focusing effect. Zn(Im)₄ was used as the model compound. The third-shell mutant data can be fitted to two Im rings at a slightly greater distance ($\approx 0.04 \text{ \AA}$) than in the model.

could functionally substitute for Cys-154, it was anticipated that the mutant E1A protein would have an HC¹⁵⁷C₂ or a C¹⁵⁷HC₂ structure. Instead, the mutant protein was converted to an H₂C₂ finger. Zn(II) is probably no longer bound to Cys-157, while the binding of Zn(II) to Cys-171 and Cys-174 is retained. Thus, it appears that the single amino acid substitution in C154S results in the abandonment of one of the normal ligands (Cys-157) and the recruitment of two nearby histidines that are otherwise not Zn(II) ligands in E1A. It is clear from these studies that, for trans-activation to occur, Zn(II) must be bound by E1A in a precise manner.

We thank Dr. Donatella Pascolini (The Wistar Institute of Anatomy and Biology, Philadelphia) and Dr. Grant Bunker (Illinois Institute of Technology, Chicago) for critical reading of the manuscript. We appreciate the support of the staff of the National Biostructures PRT and the National Synchrotron Light Source. This work was partially supported by National Institutes of Health Grants CA-29797 (to R.P.R.) and GM-28057, and National Science Foundation Grant DMB-8703990 (to F.Y.-H.W.). L.C.W. was supported by National Institutes of Health Training Grant CA-09171.

1. Evans, R. M. & Hollenberg, S. M. (1988) *Cell* **52**, 1–3.
2. Klug, A. & Rhodes, D. (1987) *Trends Biochem. Sci.* **12**, 464–469.
3. Witte, M. M. & Dickson, R. C. (1988) *Mol. Cell. Biol.* **8**, 3726–3733.
4. Johnston, M. (1987) *Nature (London)* **328**, 353–355.
5. Redeman, N., Gaul, U. & Jackle, H. (1988) *Nature (London)* **332**, 90–92.
6. Kadonaga, J. T., Carner, K. R., Masiarz, F. R. & Tjian, R. (1987) *Cell* **51**, 1079–1090.
7. Berg, J. M. (1989) *Cell* **57**, 1065–1068.
8. Miller, J., McLachlan, A. D. & Klug, A. (1985) *EMBO J.* **4**, 1609–1614.
9. Hanas, J. S., Hazuda, D. J., Bogenhagen, D. F., Wu, F. Y.-H. & Wu, C.-W. (1983) *J. Biol. Chem.* **258**, 14120–14125.
10. Parraga, G., Horvath, S. J., Eisen, A., Taylor, W. E., Hood, L., Young, E. T. & Klevit, R. E. (1988) *Science* **241**, 1489–1492.
11. Freedman, L. P., Luisi, B. F., Korszun, Z. R., Basavappa, R., Sigler, P. B. & Yamamoto, K. R. (1988) *Nature (London)* **334**, 543–546.
12. Diakun, G. P., Fairall, L. & Klug, A. (1986) *Nature (London)* **324**, 698–699.
13. Klevit, R. E., Herriott, J. R. & Horvath, S. J. (1990) *Proteins* **7**, 215–226.
14. Lee, M. S., Gippert, G. P., Soman, K. V., Case, D. A. & Wright, P. E. (1989) *Science* **245**, 635–637.
15. Hard, T., Kellenbach, E., Boelens, R., Maler, B. A., Dahlman, K., Freedman, L. P., Carlstedt-Duke, J., Yamamoto, K. R., Gustafsson, J. A. & Kaptein, R. (1990) *Science* **249**, 157–160.
16. Berk, A. J., Lee, F., Harrison, T., Williams, J. & Sharp, P. A. (1979) *Cell* **17**, 935–944.
17. Jones, N. & Shenk, T. (1979) *Proc. Natl. Acad. Sci. USA* **76**, 3665–3669.
18. Kao, H.-T. & Nevins, J. R. (1983) *Mol. Cell. Biol.* **3**, 2058–2065.
19. Stein, R. & Ziff, E. B. (1984) *Mol. Cell. Biol.* **4**, 2792–2801.
20. Engelke, D. R., Ng, S.-Y., Shastry, B. S. & Roeder, R. G. (1980) *Cell* **19**, 717–728.
21. Kadonaga, J. T. & Tjian, R. (1986) *Proc. Natl. Acad. Sci. USA* **83**, 5889–5893.
22. Eisen, A., Taylor, W. E., Blumberg, H. & Young, E. T. (1988) *Mol. Cell. Biol.* **8**, 4552–4556.
23. Nagai, K., Yukinobu, N., Nasmyth, K. & Rhodes, D. (1988) *Nature (London)* **332**, 284–286.
24. Chandler, V. L., Maler, B. A. & Yamamoto, K. R. (1983) *Cell* **33**, 489–499.
25. Ferguson, B., Krippel, B., Jones, N., Richter, J., Westphal, H. & Rosenberg, M. (1985) in *Cancer Cells*, eds. Feramisco, J., Ozanne, B. & Stiles, C. (Cold Spring Harbor Lab., Cold Spring Harbor, NY), Vol. 3, pp. 265–274.
26. Chatterjee, P. K., Bruner, M., Flint, S. J. & Harter, M. L. (1988) *EMBO J.* **7**, 835–841.
27. Glenn, G. M. & Ricciardi, R. P. (1985) *J. Virol.* **56**, 66–74.
28. Montell, C. E., Fisher, E., Caruthers, M. & Berk, A. J. (1982) *Nature (London)* **295**, 380–384.
29. Ricciardi, R. P., Jones, R. L., Cepko, C. L., Sharp, P. A. & Roberts, B. E. (1981) *Proc. Natl. Acad. Sci. USA* **78**, 6121–6125.
30. Berk, A. J. (1986) *Annu. Rev. Genet.* **20**, 45–79.
31. Pei, R. & Berk, A. J. (1989) *J. Virol.* **63**, 3499–3506.
32. Koveshki, I., Reichel, R. & Nevins, J. R. (1986) *Cell* **45**, 219–228.
33. Wu, L., Rosser, D. S. E., Schmidt, M. C. & Berk, A. J. (1987) *Nature (London)* **326**, 512–515.
34. Glenn, G. M. & Ricciardi, R. P. (1987) *Mol. Cell. Biol.* **7**, 1004–1011.
35. Liu, F. & Green, M. R. (1990) *Cell* **61**, 1217–1224.
36. Berg, J. M. (1986) *Science* **232**, 485–487.
37. Culp, J. S., Webster, L. C., Friedman, D. J., Smith, C. L., Huang, W., Wu, F. Y.-H., Rosenberg, M. & Ricciardi, R. P. (1988) *Proc. Natl. Acad. Sci. USA* **85**, 6450–6454.
38. Jones, N. C., Richter, J. D., Weeks, D. L. & Smith, L. D. (1983) *Mol. Cell. Biol.* **3**, 2131–2142.
39. Weeks, D. L. & Jones, N. C. (1983) *Mol. Cell. Biol.* **3**, 1222–1234.
40. Gorman, C. M., Moffat, L. F. & Howard, B. H. (1982) *Mol. Cell. Biol.* **2**, 1044–1051.
41. Nakamaye, K. & Eckstein, F. (1986) *Nucleic Acids Res.* **14**, 9679–9698.
42. Sanger, F., Nicklen, S. & Coulson, A. R. (1977) *Proc. Natl. Acad. Sci. USA* **74**, 5463–5467.
43. Ferguson, B., Jones, N., Richter, J. & Rosenberg, M. (1984) *Science* **224**, 1343–1346.
44. Bradford, M. (1976) *Anal. Biochem.* **72**, 248–254.
45. Stern, E. A. & Heald, S. M. (1986) in *Handbook on Synchrotron Radiation*, ed. Koch, E. (North-Holland, New York), pp. 955–1014.
46. Sayers, D. E. & Bunker, B. A. (1987) in *X-Ray Absorption: Principles, Applications, Techniques of EXAFS, SEXAFS, and XANES*, eds. Koningsberger, D. & Prins, R. (Wiley, New York), pp. 211–253.
47. Bunker, G. (1983) *Nucl. Instrum. Methods* **207**, 437–444.
48. Lee, P. A., Citrin, P. H., Eisenberger, P. & Kincaid, B. M. (1981) *Rev. Mod. Phys.* **53**, 769–806.
49. Zhang, K., Stern, E. A., Ellis, F., Sanders-Loehr, J. & Shiemke, A. K. (1988) *Biochemistry* **27**, 7470–7479.
50. Bouldin, C. (1984) Ph.D. thesis (University of Washington, Seattle).
51. Crozier, E., Rehr, J. & Ingalls, R. (1987) in *X-Ray Absorption: Principles, Applications, Techniques of EXAFS, SEXAFS, and XANES*, eds. Koningsberger, D. & Prins, R. (Wiley, New York), pp. 443–571.
52. Bunker, G., Stern, E. A., Blankenship, R. E. & Parson, W. W. (1982) *Biophys. J.* **37**, 539–542.
53. Webster, L. C. & Ricciardi, R. P. (1991) *Mol. Cell. Biol.* **11**, 4287–4296.